Published in final edited form as:
Cancer Res. 2012 April 15; 72(8): 1943–1952. doi:10.1158/0008-5472.CAN-11-1351.

Dermatan sulfate is involved in the tumorigenic properties of Esophagus Squamous Cell Carcinoma

Martin Thelin[1,#], **Katrin J. Svensson**[3], **Xiaofeng Shi**[2], **Mariam Bagher**[1], **Jakob Axelsson**[1], **Anna Isinger-Ekstrand**[4], **Toin H van Kuppevelt**[5], **Jan Johansson**[6], **Mef Nilbert**[4], **Joseph Zaia**[2], **Mattias Belting**[3,4], **Marco Maccarana**[1], and **Anders Malmström**[1]

[1]Department of Experimental Medical Science, Biomedical Center D12, Lund University, SE-221 84 Lund, Sweden [2]Department of Biochemistry, Center for Biomedical Mass Spectrometry, Boston University School of Medicine, Boston, Massachusetts 02118, USA [3]Section of Oncology, Department of Clinical Sciences, Lund University, SE-221 85, Lund, Sweden [4]Department of Oncology, Skåne University Hospital, Barngatan 2, SE-221 85 Lund, Sweden [5]Department of Biochemistry, Nijmegen Center for Molecular Life Sciences, Radboud University Nijmegen Medical Center, 6500HB Nijmegen, The Netherlands [6]Department of Surgery, Clinical Sciences, Lund University, Lund University Hospital, SE-221 85 Lund, Sweden

Abstract

Extracellular matrix, either produced by cancer cells or by cancer-associated fibroblasts, influences angiogenesis, invasion and metastasis. Chondroitin/dermatan sulfate (CS/DS) proteoglycans, which occur both in the matrix and at the cell surface, play important roles in these processes. The unique feature that distinguishes DS from CS is the presence of iduronic acid (IdoA) in DS. Here, we report that CS/DS is increased five-fold in human biopsies of esophagus squamous cell carcinoma (ESCC), an aggressive tumor with poor prognosis, as compared with normal tissue. The main IdoA-producing enzyme, DS epimerase 1 (DS-epi1), together with the 6-O- and 4-O-sulfotransferases, were highly up-regulated in ESCC biopsies. Importantly, CS/DS structure in patient tumors was significantly altered compared with normal tissue, as determined by sensitive mass spectrometry. To further understand the roles of IdoA in tumor development, DS-epi1 expression, and consequently IdoA content, was downregulated in ESCC cells. IdoA-deficient cells exhibited decreased migration and invasion capabilities in vitro, which was associated with reduced cellular binding of hepatocyte growth factor, inhibition of pERK-1/2 signaling, and de-regulated actin cytoskeleton dynamics and focal adhesion formation. Our findings demonstrate that IdoA in DS influences tumorigenesis by affecting cancer cell behavior. Therefore, down-regulation of IdoA by DS-epi1 inhibitors may represent a new anti-cancer therapy.

Keywords

Esophagus squamous cell carcinoma; dermatan sulfate; dermatan sulfate epimerase 1; iduronic acid; hepatocyte growth factor

[#]**Corresponding author**: Martin Thelin Department of Experimental Medical Science, Biomedical Center D12, Lund University, SE-221 84 Lund, Sweden; martin.thelin@med.lu.se.

INTRODUCTION

Malignant tumors of the esophagus, comprising the two dominating forms, adenocarcinoma and squamous cell carcinoma (ESCC), are the seventh leading cancer-related cause of death worldwide (1). The poor prognosis of ESCC and other types of SCC has motivated research on new treatment strategies. SCC Antigen Recognized by cytotoxic T lymphocytes 2 (SART2) was cloned as a gene with unknown functions highly expressed in SCC of different origins (2). Subsequently, a phase I clinical trial was conducted with prostate cancer patients by immunization with SART2 peptides (3). Our group found that SART2 is identical to dermatan sulfate epimerase 1 (DS-epi1), an enzyme involved in the biosynthesis of the complex polysaccharide DS (4).

CS/DS polysaccharides are unbranched polymers consisting of repeated alternating hexuronic acid (either glucuronic acid or iduronic acid; GlcA or IdoA) and *N*-acetylgalactosamime (GalNAc). DS-epi1 and 2 convert GlcA to its epimer, IdoA, to a variable degree. The presence in a chain of even a single IdoA dictates the name of DS, which is invariably composed of a mixture of the two epimers. GalNAc residues in CS/DS are almost quantitatively sulfated at the hydroxyl groups either in the C4 or C6 position (4-OS and 6-OS), or occasionally in both positions. Similarly, GlcA/IdoA can be sulfated to a certain extent at the C2 position. Four 4-*O*-sulfotransferases, three 6-*O*-sulfotransferases and a single 2-*O*-sulfotransferase catalyze the reactions. As a result of these modifications CS/DS contains structural microdomains endowed with biological information. For instance, less predominant structures containing GlcA/IdoA(2-*O*S)-GalNAC(6-*O*S) and IdoA(2-*O*S)-GalNAC(4-*O*S) are important for neurite outgrowth and coagulation, respectively (5, 6).

CS/DS proteoglycans (PGs) consist of CS/DS chains attached to different core proteins. They play a recognized role in the extracellular matrix of host organ stroma, in tumor extracellular matrix, and on the cell surface of cancer cells (7). Functions of CS/DS-PGs in tumor progression can be attributed not only to the core proteins but also to the CS/DS chains. Removal of the CS/DS chains has been demonstrated to inhibit angiogenesis, proliferation, and invasion of melanoma cells (8). GlcAGalNAC(4-*O*- and 6-*O*-disulfated)-containing CS structures on the cell surface of lung carcinoma and osteosarcoma cells are important in the metastatic process (9, 10). In addition, IdoA-containing domains bind the fibroblast growth factors, FGF2 and FGF7, and hepatocyte growth factor (HGF) (11–13). HGF, together with its receptor c-MET are major players in cancer migration and invasion (14). Fibroblast-secreted HGF was shown to promote ESCC invasion through the c-MET receptor in an *in vivo*-like organotypic 3D cell culture (15). It is known that HGF bind DS in an *in vitro* (12), but, the functions of HGF binding to DS and its possible role in cancer are still unknown.

The high expression of DS-epi1 in human SCC prompted us to analyze the amount, structure, and localization of DS in ESCCs. Further, using *in vitro* models of ESCC we aimed to elucidate whether IdoA in DS could have a functional role in critical aspects of tumor development.

MATERIALS AND METHODS

Materials, and descriptions of primary antibodies and chemicals, immunohistochemical DS-epi1 staining, characterization of metabolically labeled CS/DS chains from the cell layer and cell culture medium, immunoblot analysis and phospho-kinase array, qRT-PCR, digital holographic imaging, O-sulfotransferase assay, micro array RNA analysis and characterization of the position of the incorporated sulfates are listed in SI Materials and Methods.

Patient material

Thirty-two male and nine female patients, aged 39–83 years (mean 65 years) diagnosed with ESCC (n = 14), esophageal adenocarcinoma (n = 19), or gastric adenocarcinoma (n = 8) were randomly selected among the patients which underwent primary surgery at Lund University Hospital, Sweden, during 2001–2005 (Supplementary Table I). None of the patients had received neoadjuvant radiotherapy or chemotherapy. Biopsies were taken from the normal and carcinoma-afflicted part of the removed tissues and directly snap-frozen. Written informed consent was provided by all patients, and the study was approved by the Lund University ethics committee. Results presented in Figures 1, 5 and 6 were obtained from biopsies randomly selected among the ESCC patients.

Cell culture

TE cell lines were a gift from Dr. Dinjens, Rotterdam, The Netherlands (17). The TE-1 cell line was authenticated by short tandem repeat profiling by Boonstra et al 2007 (17). TE-1 cells were routine cultured in RPMI 1640 supplemented with 10% FBS.

DS-epimerase assay

Lysate preparation from 50–200 mg of biopsy tissues for epimerase and *O*-sulfotransferase assays was performed as described (16). Protein concentration was estimated by the Bradford assay (Bio-Rad). The first step of the epimerization reaction is the abstraction of the C5-hydrogen from the chondroitin substrate, which will subsequently form water in the reaction buffer. Epimerase assay measures the presence of $^{3}H_2O$ derived from *in vivo* labeled ^{3}H-C5 chondroitin substrate, and was performed as described previously (4).

Lentivirus-mediated gene silencing

TE-1 cells were infected according to the manufacturer's instructions, with MISSION Lentiviral Transduction Particles (SIGMA code: SHVRS) containing two shRNA sequences specific for DS-epi1 [TRCN0000121967 (shRNA-a) and TRCN0000122101 (shRNA-b)] or non-target control shRNA (SHC002V). Following selection for puromycin resistance, different isolated clones were tested for epimerase activity.

Immunocytochemistry

DS-epi1 staining was performed using immunopurified anti-DS-epi1. Briefly, TE-1 cells were grown in chamber slides, fixed with methanol for 10 min, permeabilized for 10 min in 0.2% Triton X-100, and blocked for 1 h with 5 % BSA in TBS. Immunopurified anti-DS-epi1 (2 μg/ml) and anti-GM130 (1:100) antibodies were incubated overnight at 4 °C and visualized using goat anti-rabbit IgG AF488 (Invitrogen A1100) and goat anti-mouse IgG AF546 (Invitrogen A11003), respectively, at 1:200 dilutions. The presence of IdoA on the cell surface was visualized using a single chain phage display antibody (GD3A12) that specifically recognizes DS (18). Cells were fixed with methanol for 2 min and stained as previously described by Li *et al.*, 2008 (9). Immunostaining of pFAK and F-actin was performed after a wound scratch assay in chamber slides. Cells were fixed in 4% PFA, permeabilized in Triton 0.1%, blocked in 1% BSA for 30 min and stained with anti-pY397FAK (1:1000) overnight at 4 °C in 1% BSA. pFAK was visualized with goat-anti mouse-AF488 at 1:500 dilution (Invitrogen) and subsequently counterstained with phalloidin-TRITC (P-1951, Sigma). HGF surface staining was performed according to the manufacturer's instructions followed by IdoA staining (see above). Briefly, cells were fixed in methanol, and recombinant, biotinylated HGF (1:10) was added followed by visualization with avidin-FITC (1:10). Controls without biotinylated HGF or primary anti-IdoA antibodywere included in all experiments. Cells were analyzed using a Zeiss LSM 710 confocal scanning microscope equipped with a 20× and 63× objectives.

Flow cytometry

Quantification of IdoA present at the at cell surface staining was performed after detachment of the cells using PBS supplemented with 0.5 mM EDTA. Sequential application of antibodies to DS (GD3A12; 1:80), rabbit anti-tag VSV-G (1:400), and donkey anti-rabbit IgG 488 (1:200; Jackson) was performed for 30 min at 4 °C. Human, biotinylated HGF binding experiments were performed after 24 h starvation in 0.1% serum followed by cell detachment in 2 mM EDTA/PBS and analyzed according to the protocol provided by the manufacturer. A FACS-Calibur instrument integrated with Cell-Quest software (BD Biosciences), and Flowjo were used for analysis.

In vitro wound scratch assay

TE-1 cells were grown to confluence in six-well culture plates and starved in medium supplemented with 0.1% serum for 48 h. Confluent cell monolayers were scratched and cells were washed twice followed by the addition of fresh medium supplemented with 0.1% FBS in the absence or presence of 50 ng/ml of HGF or, alternatively, 1 or 10 ng/ml of FGF2 (HGF and FGF2: Sigma H1404 and F0291, respectively). Closure of the scratch was monitored using a 4× objective at 0, 24, 48, and 72 h. Digital pictures were analyzed using AutoCad software, and scratched cell-free areas were calculated.

Migration and invasion assays

Cells were starved in 0.1% serum for 24 h, detached by 2mM EDTA/PBS, and 80,000 cells were seeded in serum free medium on 24-Transwell membranes (8 μm pores). For invasion assay, the upper side of the membrane was coated with 70 μl of 1 mg/ml Matrigel. The lower chamber was filled with medium, supplement with 0.1% FBS with or without 50 ng/ml HGF. After 48 h, membranes were fixed in 1% glutaraldehyde and stained with 0.5% crystal violet. Membranes were punched out with a 6 mm diameter dermal biopsy punch and crystal violet was solubilized in 10% acetic acid and measured. Percent of migrated cells was calculated as: absorbance 595 nm from migrated cells / absorbance 595 nm from migrated + nonmigrated cells.

Mass spectrometric analysis

Approximately 30 mg (wet weight) biopsies of normal tissue and carcinoma-afflicted tissue that also contained surrounding stroma were freeze dried and digested for 48 h at 55 °C in 50 mM Tris/HCl, pH 8, 1 mM $CaCl_2$, 1% Triton X-100, containing 0.5 mg pronase. Glycosaminoglycans (GAGs) were released by incubation of the pronase-digested tissue sample with 0.5 M NaOH at 4 °C for 24 h. The alkaline solution was neutralized to pH 6 by acetic acid and centrifuged at 11,000 × g for 10 min. The supernatants containing GAGs were recovered by a weak anion exchange workup, using 1.5 ml DEAE-Sephacel columns. Samples were loaded, and washed with 25 mL 0.1 M NaCl, 20 mM NaAc pH 6.0 buffer. GAGs were eluted with 2.5 mL of 1 M NaCl, 20 mM NaOAc pH 6.0. These fractions were desalted with PD-10 columns and vacuum dried. The exhaustive depolymerization was accomplished by dissolving one sixth of each sample in 10 μl water, followed by adding 8 μl 100 mM Tris/HCl pH 7.45 2 μl 1 M ammonium acetate, 20 mU of chondroitinase ABC, 10 mU chondroitinase AC-I, and 1.25 mU chondroitinase B. In a distinct incubation, 2 mU of chondroitinase B only was added to the GAG samples, in the presence of 0.1% BSA and 1 μM $CaCl_2$ to specifically cleave at IdoA of DSs. In both cases, the digest solutions were incubated at 37 °C, and after two hours, another aliquot of lyases was added.

The disaccharide and oligosaccharide analysis using SEC LC/MS and LC/MS/MS was performed as reported previously (19, 20). Briefly, the separation was accomplished by a Superdex Peptide (GE Healthcare) column (3.2 mm × 300 mm), with isocratic solvent

(0.016 ml/min, 12.5 mM formic acid, pH titrated to 4.4 by ammonia, in 10% acetonitrile) delivered by a Waters Acquity UPLC. The effluent was coupled with an Applied Biosystem Sciex QSTAR mass spectrometer by TurboIonSpray interface.

Statistical analysis

Student's t test and Wilcoxon signed-rank test were performed using the GraphPad Prism 5.0c software.

RESULTS

DS-epi1 is expressed in an active form in ESCC biopsies

CS has been shown to be increased in several cancer types (21), although little is known about DS, which is produced by DS-epi1 and -2, of which the former is predominant *in vivo* (16). DS-epi1 is highly expressed in SCC tumors, but in which cells is currently unknown. Immunohistochemical staining showed that DS-epi1 was expressed in normal esophageal epithelium and connective tissue as well as in cancer cells and tumor stroma (Fig. 1A–B). Specificity of the anti-DS-epi1 antibody was ascertained on DS-epi1$^{-/-}$ mouse esophagus (Fig. 1C–D) (16). Epimerase activity was subsequently measured in ESCC biopsies and compared to normal esophageal tissue derived from the same patient. We found that DS epimerase activity was 4-fold upregulated in cancer tissue as compared to normal tissue (Fig. 1E). Increased DS epimerase activity was also found in biopsies from esophageal adenocarcinoma and gastric adenocarcinoma patients (Fig. S1). Consistently, DS-epi1 protein expression was highly upregulated (Fig. 1F). At least three isoforms of DS-epi1 were present in tumor samples, possibly corresponding to differences in N-glycosylated isoforms (22), while in normal tissues, DS-epi1 was below detection level. We thus concluded that functional DS-epi1 is elevated in human ESCC.

DS-epi1 down-regulation decreases IdoA in CS/DS in the ESCC cell line TE-1

Elevated DS-epi1 levels in human ESCC prompted studies on the functional effects of DS-epi1 *in vitro*. To evaluate the role of IdoA in tumorigenesis, we made use of TE-1 cells, a well established cellular model of ESCC (15, 23, 24). TE-1 cells displayed the highest DS epimerase activity among the TE-1, -2, -4, -5, -8 cell lines tested, (Supplementary Table II). TE-1 cells were infected by lentiviruses containing two DS-epi1 shRNA sequences (shRNA-a and shRNA-b) and one control shRNA sequence. Two clones containing shRNA-a or shRNA-b were studied. Epimerase activity was downregulated by approx. 90% in shRNA-a transduced cells and approx. 82% in shRNA-b transduced cells, as compared to control non-target shRNA transduced clones (Supplementary Table II). Accordingly, DS-epi1 protein was substantially reduced in shRNA-a and shRNA-b cells (Fig. 2A). Additionally, confocal microscopy analysis demonstrated that DS-epi1 co-localized with the *cis* Golgi marker GM130 in control cells, while virtually below detection level in shRNA-a cells (Fig. 2B). To study the effect of DS-epi1 down regulation on DS structure, cells were labeled with [^{35}S]-sulfate and PGs derived either from the cell layer or released into the medium were fractionated by size exclusion chromatography. Isolated [^{35}S]-sulfate labeled CS/DS chains were specifically degraded at IdoA residues using chondroitinase B, and size fractionated (Fig. 2C). Calculation based on the degradation pattern demonstrated that the IdoA content was 7 % to 15 % in the control CS/DS-PGs, and was approx. 80 % reduced upon DS-epi1 silencing (Table I). In accordance with these results, IdoA-containing epitopes at the cell surface, measured by an anti-DS antibody, were reduced by 64 % and 47 % upon DS-epi1 downregulation by shRNA-a and shRNA-b, respectively (Fig. 2D). These data were corroborated by visualization of cell surface IdoA using an anti-DS antibody, which was substantially reduced IdoA staining was seen in DS-epi1 shRNA-a cells as compared to control cells (Fig. 2E). The remaining IdoA upon DS-epi1 downregulation could be formed

by the action of DS-epi2, the mRNA expression of which increased 5-fold in DS-epi1-downregulated cells (Fig 2G), while, as expected, DS-epi1 mRNA was decreased by approx. 90 % (Fig. 2F).

IdoA is involved in HGF-mediated ERK signaling

HGF has previously been shown to bind DS with higher affinity than CS (13). Control shRNA TE-1 cells were stained with recombinant, biotinylated HGF and anti-IdoA antibody and visualized using confocal microscopy. In support of a direct interaction of HGF with IdoA of DS, partial co-localization on the cell surface was observed (Fig. 3A), and HGF binding was significantly reduced in shRNA-a and shRNA–b cells, as compared to control shRNA cells (Fig 3B). Notably, these cells expressed equal amounts of the MET receptor, which supports a direct role of IdoA in HGF binding (Fig. 3C).

To further address the signaling pathways activated by HGF in TE-1 cells, we initially performed a phosphokinase antibody array on shRNA control cells with or without HGF stimulation (Fig. 3D). HGF appeared to specifically induce phosphorylation of ERK-1/2 and its downstream target RSK-1/2/3 under the conditions used. HGF-mediated induction of pERK-1/2 was confirmed by Western blotting and, more importantly, the induction was substantially reduced in shRNA-a and shRNA-b cells as compared with control shRNA cells (Fig. 3E). These data indicate that unperturbed IdoA formation is required for efficient HGF-mediated signaling through ERK-1/2 in TE-1 cells.

Cancer cell migration and invasion depend on IdoA

To investigate possible functional roles of IdoA, we next performed migration and invasion assays with shRNA control and shRNA-a and shRNa-b TE-1 cells. In a wound scratch assay, the capacity of control cells to migrate was greatly enhanced by the addition of HGF (Fig. 4A–B). On the contrary, FGF2 added at 1 or 10 ng/ml did not stimulate migration of TE-1 cells (data not shown). Interestingly, shRNA-a and shRNA–b cells were found to migrate significantly less than shRNA control cells, and this difference was more pronounced in the context of HGF stimulation (Fig. 4A–B). Migration and invasion were next studied in transwell assays and, again, HGF increased TE-1 cell migration (Fig. 4C), although to a lesser extent than in wound scratch experiments. ShRNA-a and shRNA-b cells presented significant reduction in migration as compared to control cells, both in the absence and in the presence of HGF. Control cell invasion was enhanced approx. 2-fold by the addition of HGF, and shRNA-a cells had significantly reduced the invasive capacity of TE-1 cells in the context of HGF stimulation ($p < 0.01$), whereas with border-line significance ($p = 0.051$) in non-stimulated cells (Fig. 4D). ShRNA-b, however, had no effect on the invasion of non-stimulated cells, whereas there was a strong trend ($p = 0.054$) towards inhibition of HGF-driven invasion of TE-1 cells (Fig. 4D). Cell migration requires a continuous cycle of protrusion, attachment, and traction at the leading edge that depends on the coordinated dynamics of the actin cytoskeleton and focal adhesions (25). Indeed, IdoA was found to have a role in cell attachment and spreading, as well as in cytoskeleton dynamics; shRNA-a cells exhibited an approx. 40% greater cell area compared to control shRNA cells (Fig. S2B), which was associated with an approx. 2-fold induction of p-FAK and total FAK as compared with control cells (Fig. 4E). Moreover, p-FAK appeared to be increased and more homogeneously distributed at the cell membrane as compared with control cells in shRNA-a and shRNA-b cells after 48 h of HGF stimulation in a wound scratch assay (Fig. 4F). Further, DS-epi1-downregulated shRNA-a and shRNA-b cells displayed an altered morphology with less prominent plasma membrane protrusions (Fig. 4F, upper panel), and with relatively few cytoplasmic stress fibers compared to control cells (Fig. S2C). In conclusion, these data show that cell surface located IdoA is involved in the migratory and invasive behavior of ESCC cells, especially in the context of HGF signaling,

and suggest a novel role of DS-epi1 in the regulation of cell motility and cytoskeleton modulation.

ESCC tumors express an altered CS/DS structure as compared to normal tissue

Experimental studies, including the data presented above, clearly indicate that the biological functions of CS/DS chains depend on their fine structure. However, clinical data are still lacking to date to extend the validity of these *in vitro* experiments. For the first time, we have investigated the structure of CS/DS chains derived from small amounts of pathological samples using a sensitive mass spectrometric approach. To this end, CS/DS was purified and extensively degraded into disaccharides by a mixture of chondroitinases ABC, AC-I, and B enzymes. Interestingly, sulfated disaccharides were increased 5-fold in ESCC patient tumors compared to their normal counterparts (Fig. 5A). We further analyzed the type of sulfation on the disaccharides. Normal tissues contained approx. 82 % mono sulfated, 4-*O*-sulfated disaccharides and 18 % mono sulfated, 6-*O*-sulfated disaccharides, whereas cancer tissues contained approx. 65 % mono sulfated, 4-*O*-sulfated disaccharides and 35 % mono sulfated, 6-*O*-sulfated disaccharides (Fig. 5B). Disulfated disaccharides within CS/DS chains are less abundant components that have been associated with biological functions. We present data showing that these disaccharides represented approx. 7 % of the total sulfated disaccharides in normal esophageal tissues. Their relative content in all cancer biopsies decreased approx. 4-fold compared to normal tissues (Fig. 5C).

Next, CS/DS was digested by chondroitinase B alone, resulting in disaccharides from DS regions containing at least two adjacent IdoA residues. The absolute content of IdoA disaccharides was unaffected in cancer biopsies compared to normal tissues (amount of IdoA/weight of tissue; Fig 5D). However, there was a 5-fold increase of CS/DS content in tumor tissues (Fig 5A). Collectively, these data show that the relative amount of IdoA/chain (% of IdoA / IdoA + GlcA) decreased in tumor compared to control tissues. In summary, total CS/DS levels were increased in ESCC samples. The average structure of the chains derived from tumor tissues was altered; 6-monosulfated disaccharides were increased, and 4-*O*-monosulfated as well as disulfated disaccharides and IdoA-containing structures were decreased.

Increased *O*-sulfotransferase activities in ESCC biopsies

There are three major 4-*O*- and two 6-*O*-sulfotransferases that add a sulfate group at the C4 and C6 positions of the GalNAc residue, respectively (26, 27). The activities of these sulfotransferases were measured by incubating tissue extracts with the substrates chondroitin [$(GlcA\text{-}GalNAc)_n$] or dermatan [$(IdoA\text{-}GalNAc)_n$] together with the labeled sulfate donor [^{35}S]-PAPS. The incubations with chondroitin (Fig. 6A) showed a 13-fold up-regulation of 4-*O*-activity in tumor tissue as compared to normal tissue ($p = 0.043$), while the 6-*O*-activity was increased 4-fold ($p = 0.08$). These assays measure 4- and 6-*O*-sulfotransferases activities but not DS 4-*O*-sulfotransferase 1 (D4ST-1) activity, which requires dermatan as substrate. D4ST-1 activity was upregulated in 3 out of 4 patients (Fig. 6B). Moreover, 6-*O*-sulfation, carried out by C6ST1 (27), was also detected on dermatan and increased in 3 patients out of 4. Next, CS/DS biosynthetic enzymes, beyond the epimerases and O-sulfotransferases, were analyzed using cDNA microarray (Fig. S3; the data obtained have been deposited in the Gene Expression Omnibus (GEO) database, accession number GSE27040). The mRNA levels in ESCC biopsies were compared to a reference pool of 10 human cancer cell lines to give a broad representation of transcripts. Therefore, the values do not represent a comparison between cancer and normal tissues. The data showed that tumors from 37 patients with esophageal and gastric carcinomas had similar mRNA expression patterns. Altogether, the activity results showed that the main O-sulfotransferase

activities are upregulated in human ESCC, which is in line with the increased production of CS/DS observed in tumors.

DISCUSSION

The main finding of this report is that tumor-promoting functions can be attributed to IdoA in DS chains. DS-epi1 and 2 are the enzymes responsible for conversion of GlcA to IdoA, and ultimately for the formation of DS. DS-epi1 is the main enzyme *in vivo* (16) and, because of its overexpression in most cancers, it has been suggested to be a cancer-associated antigen (2). In support of this idea, we found that DS-epi1 is highly expressed in ESCC cancer cells together with greater amounts of enzyme and increased DS-epimerase activity in cancer tissue as compared with normal tissue. Interestingly, we provide evidence that DS-associated IdoA appears to have a functional role in cancer cell behavior. Previous data suggest a synergistic effect of exogenously added DS and HGF in the stimulation of muscle cell proliferation and migration (28). The profound action of HGF on invasion has been demonstrated in a variety of cancer cells, including ESCC (15). DS and HGF could potentially form a receptor binding signaling complex in analogy with FGF2 and heparan sulfate (29, 30). Previous reports with different cell lines have shown that migration and invasion are enhanced in the presence of HGF, through its downstream target pERK-1/2 (14). Here, we demonstrate partial cell surface co-localization between HGF and IdoA, significantly reduced binding of HGF in DS-epi1-downregulated, IdoA-deficient cells, and a strong dependence on unperturbed IdoA formation for efficient HGF-mediated signaling through ERK-1/2. These effects were associated with less migration and invasion of DS-epi1-downregulated cells compared to control cells, especially in the context of HGF stimulation. It is noteworthy that a single IdoA appears to be sufficient for HGF binding to DS chains (12). Our findings that IdoA-deficient cells displayed only limited reduction of HGF binding (Fig. 3B), and more substantial reduction of HGF signaling (Fig. 3E) as well as inhibition of functional effects (Fig. 4), underscore the biological relevance of the DS-bound HGF subfraction. It may be speculated that although HGF binding remains relatively intact upon IdoA deficiency, HGF is presented in an altered microenvironment and conformation that does not allow efficient down-stream signaling activation.

Migration and invasion are intriguing processes with constant formation and disassembly of adhesion. Adhesion occurs at protrusions while disassembly of the focal adhesion complex takes place at the cell rear and at the base of protrusions. Focal adhesion kinase (FAK) is an important regulator of cytoskeleton dynamics involved in adhesion and migration (31). Our results suggest that DS-epi1-downregulated cells have a malfunctioning disassembly of adhesion complexes, and abnormal actin cytoskeleton architecture. The induction of FAK and pFAK could be due to increased spreading of IdoA-deficient cells (32). Altered signals could originiate from a modified ECM, deposite by shRNA-a and –b cells over the time of cultivation. The actual presence of IdoA in CS/DS or CS has been overlooked in many cases, especially when considering cell surface bound PGs. An exception is the part time PG CD44 that has been shown to contain IdoA under certain circumstances (33). CD44 is localized in the focal adhesions of invadopodia (34) and has a functional role in the anchoring of cytoskeleton elements to cell membrane in connection with ECM molecules, and in concentrating metalloproteases. In conclusion, the altered distribution of actin cytoskeleton and focal adhesions demonstrated in DS-epi1-downregulated cells is consistent with decreased directionality in cellular movements. Future studies clearly have to elucidate which type of PG/PGs that are specifically involved in these functions.

The changed composition and structures of CS/DS polysaccharide chains in malignant tumors could play distinct roles in tumor development (7, 35). We found that the expression patterns of CS/DS biosynthetic enzymes and the structure of the CS/DS chains are consistent

among the patients examined. In ESCC biopsies, the activities of epimerases, 4-O- and 6-*O*-sulfotransferases were increased. It is plausible that these activities are needed to stand the 5-fold increase in CS/DS production. Previous studies have shown that CS/DS increases in most of the cancers examined (21, 36). We extend previous data and show that the average composition of CS/DS chains produced by tumor biopsies is altered in many different aspects as compared to normal tissues. IdoA residues can be found in CS/DS chains in three major patterns: Isolated, where IdoA is surrounded by GlcA; in alternating IdoA-GlcA structures; or in long blocks of adjacent IdoA residues. Using mass spectrometry analysis of isolated CS/DS, we reveal that the relative content of IdoA is decreased in blocks and in alternating structures. Intriguingly, there is thus an apparent discrepancy between higher epimerase activity in tumor tissue and lower relative content of alternating and blocks of IdoA structures. This discrepancy could simply be explained by the presence of isolated IdoA structures that were not included in the mass spectrometry analyses. Alternatively, induction of the turnover of IdoA-containing DS oligosaccharides in tumors may cause the release of sequestered HGF and additional growth factors from CS/DS PGs in the stroma resulting in increased accessibility to and stimulation of tumor cells.

In summary, we show that critical aspects of cancer cell function are dependent on the presence of IdoA in DS, and specific features of the CS/DS structure are altered in ESCC patient tumors. This work demonstrates the potential to pharmalogically block DS-epi1 and expectably down-regulate HGF signaling, which may provide new avenues for cancer treatment.

Supplementary Material

Refer to Web version on PubMed Central for supplementary material.

Acknowledgments

We thank Lena M. Svensson for useful discussions.

Grant support: Grants to M.T., M.B., M.M., and A.M. were from the Swedish Research Council, the Gunnar Nilsson foundation, and the Medical faculty of Lund. X.S. and J.Z. were supported by NIH grants P41RR10888 and R01098950.

REFERENCES

1. Jemal A, Siegel R, Ward E, Murray T, Xu J, Thun MJ. Cancer statistics, 2007. CA Cancer J Clin. 2007; 57:43–66. [PubMed: 17237035]
2. Nakao M, Shichijo S, Imaizumi T, Inoue Y, Matsunaga K, Yamada A, et al. Identification of a gene coding for a new squamous cell carcinoma antigen recognized by the CTL. J Immunol. 2000; 164:2565–74. [PubMed: 10679095]
3. Noguchi M, Kobayashi K, Suetsugu N, Tomiyasu K, Suekane S, Yamada A, et al. Induction of cellular and humoral immune responses to tumor cells and peptides in HLA-A24 positive hormone-refractory prostate cancer patients by peptide vaccination. Prostate. 2003; 57:80–92. [PubMed: 12886526]
4. Maccarana M, Olander B, Malmstrom J, Tiedemann K, Aebersold R, Lindahl U, et al. Biosynthesis of dermatan sulfate: chondroitin-glucuronate C5-epimerase is identical to SART2. J Biol Chem. 2006; 281:11560–8. [PubMed: 16505484]
5. Sugahara K, Mikami T. Chondroitin/dermatan sulfate in the central nervous system. Curr Opin Struct Biol. 2007; 17:536–45. [PubMed: 17928217]
6. Tollefsen DM. Vascular dermatan sulfate and heparin cofactor II. Prog Mol Biol Transl Sci. 2010; 93:351–72. [PubMed: 20807652]
7. Wegrowski Y, Maquart FX. Chondroitin sulfate proteoglycans in tumor progression. Adv Pharmacol. 2006; 53:297–321. [PubMed: 17239772]

8. Denholm EM, Lin YQ, Silver PJ. Anti-tumor activities of chondroitinase AC and chondroitinase B: inhibition of angiogenesis, proliferation and invasion. Eur J Pharmacol. 2001; 416:213–21. [PubMed: 11290371]
9. Li F, Ten Dam GB, Murugan S, Yamada S, Hashiguchi T, Mizumoto S, et al. Involvement of highly sulfated chondroitin sulfate in the metastasis of the Lewis lung carcinoma cells. J Biol Chem. 2008; 283:34294–304. [PubMed: 18930920]
10. Basappa, Murugan S, Sugahara KN, Lee CM, ten Dam GB, van Kuppevelt TH, et al. Involvement of chondroitin sulfate E in the liver tumor focal formation of murine osteosarcoma cells. Glycobiology. 2009; 19:735–42. [PubMed: 19293233]
11. Taylor KR, Rudisill JA, Gallo RL. Structural and sequence motifs in dermatan sulfate for promoting fibroblast growth factor-2 (FGF-2) and FGF-7 activity. J Biol Chem. 2005; 280:5300–6. [PubMed: 15563459]
12. Deakin JA, Blaum BS, Gallagher JT, Uhrin D, Lyon M. The binding properties of minimal oligosaccharides reveal a common heparan sulfate/dermatan sulfate-binding site in hepatocyte growth factor/scatter factor that can accommodate a wide variety of sulfation patterns. J Biol Chem. 2009; 284:6311–21. [PubMed: 19114710]
13. Catlow KR, Deakin JA, Wei Z, Delehedde M, Fernig DG, Gherardi E, et al. Interactions of hepatocyte growth factor/scatter factor with various glycosaminoglycans reveal an important interplay between the presence of iduronate and sulfate density. J Biol Chem. 2008; 283:5235–48. [PubMed: 18156180]
14. Trusolino L, Bertotti A, Comoglio PM. MET signalling: principles and functions in development, organ regeneration and cancer. Nat Rev Mol Cell Biol. 2010; 11:834–48. [PubMed: 21102609]
15. Grugan KD, Miller CG, Yao Y, Michaylira CZ, Ohashi S, Klein-Szanto AJ, et al. Fibroblast-secreted hepatocyte growth factor plays a functional role in esophageal squamous cell carcinoma invasion. Proc Natl Acad Sci U S A. 2010; 107:11026–31. [PubMed: 20534479]
16. Maccarana M, Kalamajski S, Kongsgaard M, Magnusson SP, Oldberg A, Malmstrom A. Dermatan sulfate epimerase 1-deficient mice have reduced content and changed distribution of iduronic acids in dermatan sulfate and an altered collagen structure in skin. Mol Cell Biol. 2009; 29:5517–28. [PubMed: 19687302]
17. Boonstra JJ, van der Velden AW, Beerens EC, van Marion R, Morita-Fujimura Y, Matsui Y, et al. Mistaken identity of widely used esophageal adenocarcinoma cell line TE-7. Cancer Res. 2007; 67:7996–8001. [PubMed: 17804709]
18. Ten Dam GB, Yamada S, Kobayashi F, Purushothaman A, van de Westerlo EM, Bulten J, et al. Dermatan sulfate domains defined by the novel antibody GD3A12, in normal tissues and ovarian adenocarcinomas. Histochem Cell Biol. 2009; 132:117–27. [PubMed: 19360434]
19. Shi X, Zaia J. Organ-specific heparan sulfate structural phenotypes. J Biol Chem. 2009; 284:11806–14. [PubMed: 19244235]
20. Staples GO, Shi X, Zaia J. Glycomics Analysis of Mammalian Heparan Sulfates Modified by the Human Extracellular Sulfatase HSulf2. PLoS One. 2011; 6:e16689. [PubMed: 21347431]
21. Theocharis AD, Tsolakis I, Tzanakakis GN, Karamanos NK. Chondroitin sulfate as a key molecule in the development of atherosclerosis and cancer progression. Adv Pharmacol. 2006; 53:281–95. [PubMed: 17239771]
22. Pacheco B, Maccarana M, Goodlett DR, Malmstrom A, Malmstrom L. Identification of the active site of DS-epimerase 1 and requirement of N-glycosylation for enzyme function. J Biol Chem. 2009; 284:1741–7. [PubMed: 19004833]
23. Faried A, Faried LS, Kimura H, Nakajima M, Sohda M, Miyazaki T, et al. RhoA and RhoC proteins promote both cell proliferation and cell invasion of human oesophageal squamous cell carcinoma cell lines in vitro and in vivo. Eur J Cancer. 2006; 42:1455–65. [PubMed: 16750623]
24. Imsumran A, Adachi Y, Yamamoto H, Li R, Wang Y, Min Y, et al. Insulin-like growth factor-I receptor as a marker for prognosis and a therapeutic target in human esophageal squamous cell carcinoma. Carcinogenesis. 2007; 28:947–56. [PubMed: 17183068]
25. McLean GW, Carragher NO, Avizienyte E, Evans J, Brunton VG, Frame MC. The role of focal-adhesion kinase in cancer - a new therapeutic opportunity. Nat Rev Cancer. 2005; 5:505–15. [PubMed: 16069815]

26. Mikami T, Mizumoto S, Kago N, Kitagawa H, Sugahara K. Specificities of three distinct human chondroitin/dermatan N-acetylgalactosamine 4-O-sulfotransferases demonstrated using partially desulfated dermatan sulfate as an acceptor: implication of differential roles in dermatan sulfate biosynthesis. J Biol Chem. 2003; 278:36115–27. [PubMed: 12847091]
27. Kitagawa H, Fujita M, Ito N, Sugahara K. Molecular cloning and expression of a novel chondroitin 6-O-sulfotransferase. J Biol Chem. 2000; 275:21075–80. [PubMed: 10781596]
28. Villena J, Brandan E. Dermatan sulfate exerts an enhanced growth factor response on skeletal muscle satellite cell proliferation and migration. J Cell Physiol. 2004; 198:169–78. [PubMed: 14603519]
29. Yayon A, Klagsbrun M, Esko JD, Leder P, Ornitz DM. Cell surface, heparin-like molecules are required for binding of basic fibroblast growth factor to its high affinity receptor. Cell. 1991; 64:841–8. [PubMed: 1847668]
30. Delehedde M, Lyon M, Gallagher JT, Rudland PS, Fernig DG. Fibroblast growth factor-2 binds to small heparin-derived oligosaccharides and stimulates a sustained phosphorylation of p42/44 mitogen-activated protein kinase and proliferation of rat mammary fibroblasts. Biochem J. 2002; 366:235–44. [PubMed: 12000311]
31. Tomar A, Schlaepfer DD. Focal adhesion kinase: switching between GAPs and GEFs in the regulation of cell motility. Curr Opin Cell Biol. 2009; 21:676–83. [PubMed: 19525103]
32. Richardson A, Malik RK, Hildebrand JD, Parsons JT. Inhibition of cell spreading by expression of the C-terminal domain of focal adhesion kinase (FAK) is rescued by coexpression of Src or catalytically inactive FAK: a role for paxillin tyrosine phosphorylation. Mol Cell Biol. 1997; 17:6906–14. [PubMed: 9372922]
33. Clark RA, Lin F, Greiling D, An J, Couchman JR. Fibroblast invasive migration into fibronectin/fibrin gels requires a previously uncharacterized dermatan sulfate-CD44 proteoglycan. J Invest Dermatol. 2004; 122:266–77. [PubMed: 15009704]
34. Weaver AM. Invadopodia: specialized cell structures for cancer invasion. Clin Exp Metastasis. 2006; 23:97–105. [PubMed: 16830222]
35. Timar J, Lapis K, Dudas J, Sebestyen A, Kopper L, Kovalszky I. Proteoglycans and tumor progression: Janus-faced molecules with contradictory functions in cancer. Semin Cancer Biol. 2002; 12:173–86. [PubMed: 12083848]
36. Theocharis AD, Vynios DH, Papageorgakopoulou N, Skandalis SS, Theocharis DA. Altered content composition and structure of glycosaminoglycans and proteoglycans in gastric carcinoma. Int J Biochem Cell Biol. 2003; 35:376–90. [PubMed: 12531251]

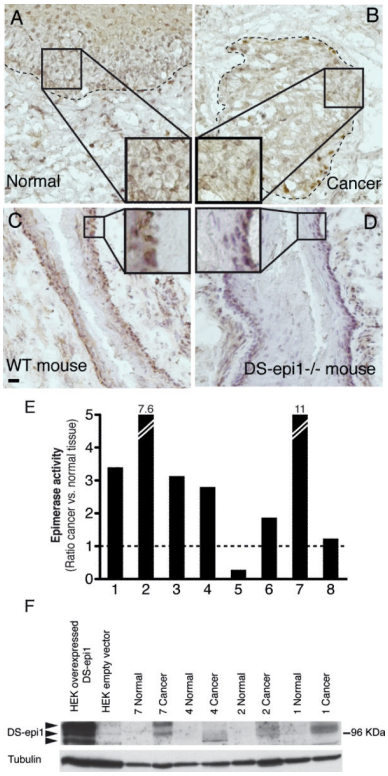

Figure 1. Active DS-epi1 is overexpressed in ESCC biopsies

A–B, normal or tumor tissue biopsies from patients were stained with anti-DS-epi1 antibody. D*otted line* marks the boundary between cancer cells and the surrounding tissue. *C–D*, mouse wild-type and DS-epi1$^{-/-}$ esophagi (16) were stained to verify the specificity of the anti-DS-ep1 antibody. Scale bar: 20 μm. *E*, cellular enzymes were detergent-extracted from biopsies, and DS-epimerase activity was measured. Epimerase specific activity in the 8 samples from normal esophagi was 117 ± 69 dpm/h/mg (^{3}H dpm released from the substrate/h/mg of assayed protein; mean ± SD; * $p < 0.05$ cancer versus normal). *F*, DS-epi1 was detected by WB in lysates from biopsies. HEK 293 cell lysates transfected with an empty vector or a vector containing DS-epi1 were included as negative and positive controls, respectively. An immunopurified anti-DS-epi1 antibody was used at 4 μg/ml.

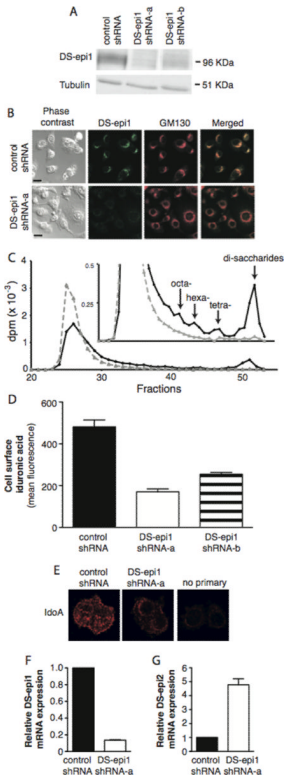

Figure 2. Down-regulation of DS-epi1 in ESCC TE-1 cells results in decreased IdoA

TE-1 cells were infected with lentiviral particles containing DS-epi1 shRNA-a, shRNA-b, or non-target control sequences. *A*, DS-epi1 protein in control, DS-epi1 shRNA-a, and shRNA–b cell lysates. Immunopurified anti-DS-epi1 antibody was used at 1 μg/ml. *B*, confocal microscopy immunofluorescence analysis of DS-epi1 (green) and the cis Golgi marker GM130 (red) shows reduced DS-epi1 levels in shRNA-a cells as compared with control. Scale bar: 20 μm. *C*, size distribution on Superdex Peptide column of metabolically labeled CS/DS chains from TE-1 cells transduced with shRNA control (black line) or DS-epi1 shRNA-a (grey, broken line) and cleaved at IdoA residues by chondroitinase B prior to column separation. CS/DS derived from the large PG versican released into the medium is shown. Two shRNA-a clones were isolated and gave similar results (one is shown for brevity). Similar patterns were obtained from the CS/DS chains of the small PGs decorin and biglycan and from PGs present in the cell layer (see Table I). *D*, surface staining of non-permeabilized TE-1 cells with the anti-DS antibody GD3A12 that specifically recognizes IdoA residues. The bars indicate mean ± SD of triplicate stainings from flow cytometry analyses. *E*, confocal microscopy immunofluorescence analysis of IdoA from a similar experiment as in (*D*). *F–G*, qRT-PCR of DS-epi1 (*F*) and DS-epi2 (*G*) on DS-epi1 shRNA-a and control shRNA cells.

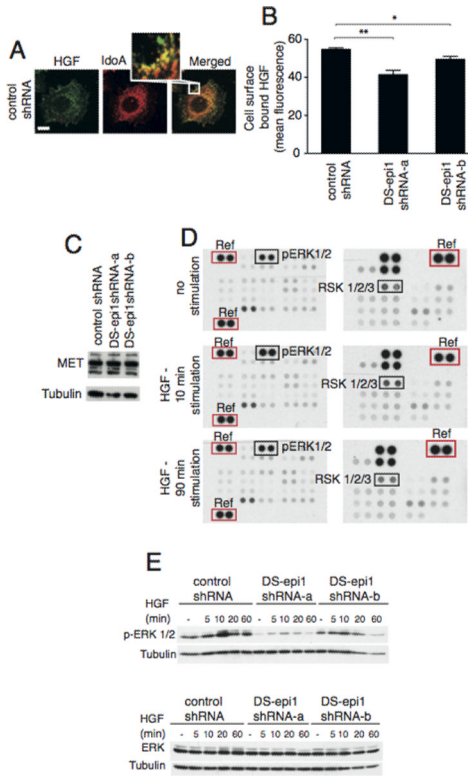

Figure 3. IdoA is involved in cellular HGF binding and HGF-dependent induction of ERK-1/2 signaling

A, confocal microscopy analysis of surface-bound recombinant, biotinylated-HGF (green) and IdoA (red) shows partial co-localization (yellow) in shRNA control cells. Scale bar: 10 μm. *B*, quantification by FACS of binding of exogenously added HGF. Shown are representative data from three independent experiments. Student's t-test was used to test the significance of differences between control and DS-epi1 down-regulated cells (* $p < 0.05$, ** $p < 0.01$). *C*, cells were lysed after 24 h starvation in 0.1% FBS and analyzed for MET protein by WB. *D*, HGF-mediated induction of pERK-1/2 in control cells. Cells were incubated with or without HGF (2.5 ng/ml) and levels of phosphorylated kinases were determined by antibody array analysis as described in SI Material and Methods. *E*, lysates from control and DS-epi1 shRNA transduced cells were prepared following incubations in the presence or absence of HGF (2.5 ng/ml) at the indicated time points, and analyzed by WB. Anti-pERK-1/2 (upper panel) and anti-ERK-1/2 (lower panel) antibodies were used at 1:2,000 and 1:1,000 dilutions, respectively.

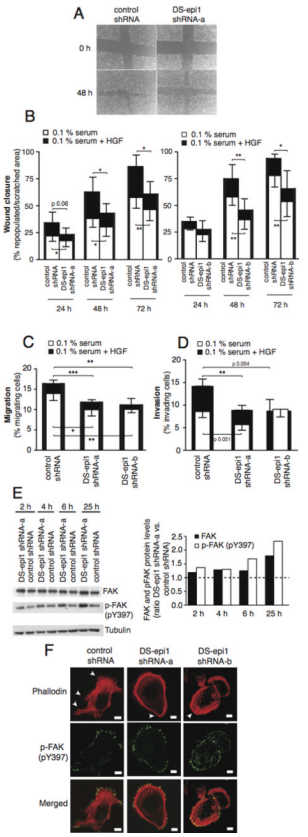

Figure 4. DS-epi1 is involved in the migration and invasion of TE-1 cells

A–B, wound scratch assay. *A*, representative phase contrast images taken with a 40× objective. *B*, quantification of the migrated area as shown in (*A*). *C*, transwell migration assay. *D*, transwell invasion assay using a Matrigel-coated membrane. *A–D*, each assay was performed in 4–6 replicates, and was repeated at least twice with similar results. *Black bars* refer to experiments in the presence of HGF (50 ng/ml). *White bars* refer to experiments without HGF. Student's t-test was used to test the significance of the differences between control and DS-epi1 down-regulated cells. (* $p < 0.05$, ** $p < 0.01$, ***$p < 0.001$) *E*, cellular lysates were prepared at the indicated time points after cell plating, and analyzed by WB. Anti-FAK and anti-pY397FAK antibodies were used at 1:4,000 and 1:1,000, respectively. Right panel: FAK/tubulin and pFAK/tubulin ratios were calculated by densitometric analysis of WB films using Quantity One. *F*, cells migrating in the wound scratch assay in the presence of HGF (50 ng/ml) were stained for actin filaments by phalloidin (red) and for focal adhesions by anti-pY397FAK (green). Scale bars, 10 μm. White arrow-heads in upper panels indicate plasma membrane protrusions.

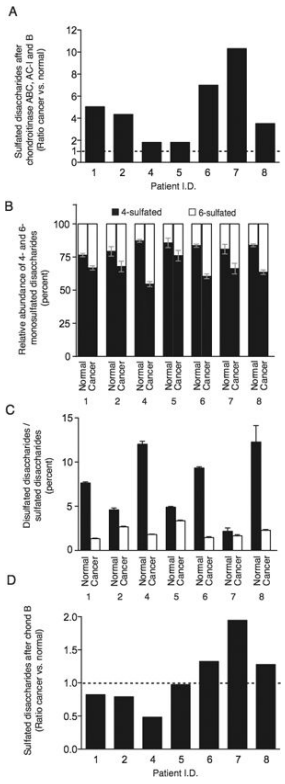

Figure 5. Mass spectrometry analysis of CS/DS from human ESCC biopsies and normal tissue

CS/DS was purified from ESCC biopsies and adjacent normal tissue and extensively degraded by a mixture of chondroitinases ABC, AC–I, and B (*A–C*), or specifically degraded at IdoA residues by chondroitinase B alone (*D*), as described in SI Material and Methods. The degradation products were separated by size permeation and on-line injected into the mass spectrometer. Monosulfated (m/z = 458) and disulfated (m/z = 538) disaccharides were quantified. Non sulfated disaccharides (m/z = 378) were not considered due to contamination from hyaluronic acid-derived disaccharides after chondroitinase ABC digestion, and as they constituted a minor component (mean 1.8%) of the predominant monosulfated disaccharides after chondroitinase B alone digestion. Measurements were performed in triplicate. P-values were obtained by Wilcoxon signed-rank test (*A–D* * $p < 0.05$ cancer versus normal). Results from analyses of normal tissue were set to 1 in *A* and *D*.

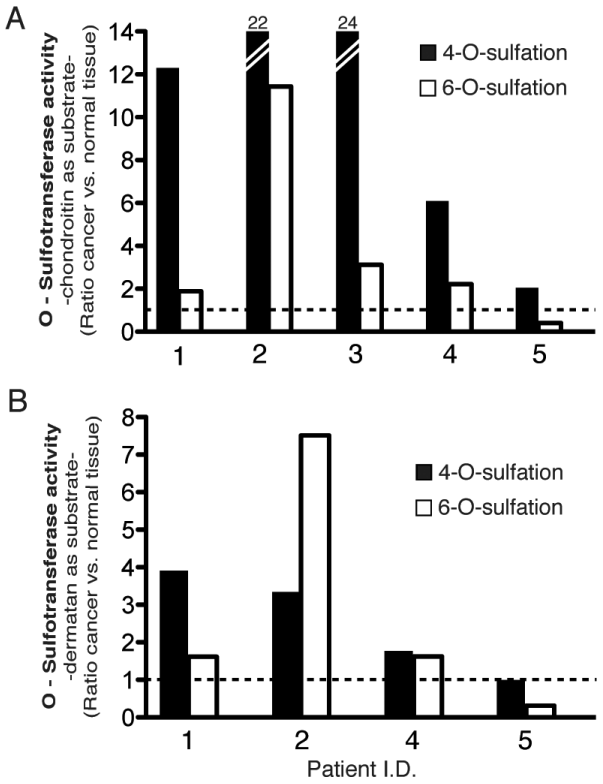

Figure 6. Increased *O*-sulfotransferase activities in ESCC tumors

Cellular enzymes were detergent-extracted from biopsies, and *O*-sulfotransferase activities adding a sulfate group to chondroitin (*A*) or dermatan (*B*) as substrates, were measured. The labeled products were recovered and quantitatively depolymerized to disaccharides by the action of chondroitinase ABC. The 6-*O*- or 4-*O*-position of the added labeled sulfate was determined by HPLC separation of the disaccharides. No labeled disulfated or 2-*O*-monosulfated disaccharides were observed (data not shown). The data are presented as the ratio of tumor versus normal tissue biopsies (set to 1), both obtained from the same patient. 4-*O*-sulfotransferase specific activity on chondroitin in normal esophagi tissues was 2,919 ± 1,458 dpm/h/mg (^{35}S incorporated into chondroitin/h/mg of assayed protein; mean ± SD). Assays were run in triplicates. P-values were obtained by subjecting the ratio values to Wilcoxon signed-rank test. Ratio of 4-*O*-sulfotransferase and 6-*O*-sulfotransferase activities on chondroitin had p-values of p=0.043 and p=0.08, respectively, when comparing tumor versus normal tissues. Ratio of sulfotransferases activites on dermatan did not reach statistical significance when comparing tumor versus normal.

Table I

IdoA content in CS/DS-PGs produced by control and DS-epi1 down-regulated TE-1 clones.

	Cell layer		Medium	
	Large	Small	Large	Small
Clones	**CS/DS PGs**	**CS/DS PGs**	**CS/DS PGs**	**CS/DS PGs**
	% iduronic acid / (iduronic acid + glucuronic acid)			
control shRNA clone 1	11,1	15,4	13,3	14,3
control shRNA clone 2	6,8	8,8	9,4	n.d.
DS-epi1 shRNA-a clone 1	2,6	2,2	2,1	3,9
DS-epi1 shRNA-a clone 2	1,7	1,4	2,6	2,6

n.d. = not determined

CS/DS-PGs were separated by gel permeation chromatography and their CS/DS chains were further purified. IdoA content is calculated from the size distribution analysis after chondroitinase B digestion, as shown in Fig. 2C.